Differential Detection for Nanoplasmonic Resonance Sensors

Joanna Ptasinski, Lin Pang, Pang-Chen Sun, Boris Slutsky, and Yeshaiahu Fainman, *Fellow, IEEE*

***Abstract*—A differential measurement design employing two nearly collinear optical beams can lead to surface plasmon polariton (SPP) sensors of increased dynamic range and signal-to-noise ratio. We demonstrate a differential measurement device that is based on wavelength interrogation, employs a single incident polarization state, and is combined with a 2-D nanohole array for operation at near-normal incidence, where this approach offers a decrease in the measurement time.**

***Index Terms*—Bioplasmonics, biosensors, gold nanohole array, surface plasmon polariton (SPP), surface plasmon resonance (SPR).**

I. Introduction

THE development of disease-related biomarker panels will require fast and efficient methods for obtaining multiparameter protein profiles [1]. Commonly used fluorescent labeling processes are easy to implement, but they disrupt the accurate measurement of kinetic constants and can lead to antibody cross-reactivity problems [2]. An alternative, label-free biodetection method utilizes the phenomenon of surface plasmon polariton (SPP) resonance. SPP based devices integrate microfluidic channels with metal-dielectric layer chips, and measure transmittance or reflectance of light, hereafter referred to as Device Transfer Function (DTF), at the metal-fluid interface [3]. The DTF exhibits a sharp resonant feature when the probe wavelength and the angle of incidence satisfy the condition for SPP excitation. The location of the resonance depends on the refractive index of the fluid, and therefore informs on its biochemical composition. The SPP-based techniques are broadly classified into wavelength interrogation, angular interrogation, and intensity interrogation families [4]–[6]. In wavelength (angular) interrogation, multiple measurements of the DTF are made at different wavelengths (respectively, angles of incidence), such that the location of the resonance may be identified by a curve fit [Fig. 1(a), shift in point A to A']. The intensity interrogation method relies on a single measurement at a fixed angle and wavelength [Fig. 1(a), shift in points B to B' or C to C']. Intensity interrogation devices are thus simpler than wavelength and angular interrogation devices, but typically less accurate. This is because changes of the magnitude and width of the DTF cannot be distinguished from a change in its location [7].

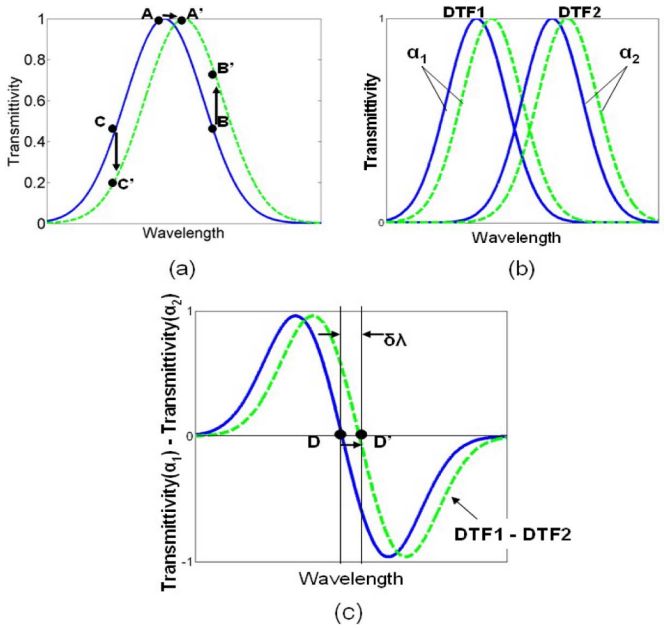

Fig. 1. (a) Typical SPR schemes determine the location of the resonance by monitoring a shift in point A to A' or they monitor the shift in intensity at a single wavelength/angle value B to B' or C to C'. (b) In differential detection the DTFs are constructed at different angles of incidence $\alpha 1$ and $\alpha 2$, such that they overlap at their FWHM. When the refractive index changes both DTFs shift in the same direction. (c) A difference of the two DTFs overlapped at their FWHM allows for an extension of the dynamic range.

Here, we describe a differential intensity interrogation method, where two measurements of the DTF are made simultaneously at nearly equal incident angles, and their difference is constructed [Fig. 1(b) and (c)]. The zero-crossing of the difference signal can be tracked with a tunable light source in a closed-loop system, similarly to the way in which beam position is tracked using quadrant detectors, resulting in a robust measurement. Closed-loop tracking of the zero crossing is performed continuously and does not require an end-to-end wavelength sweep for each measurement. Our device also utilizes a metal film perforated with a 2-D array of nanoholes, as in Tetz *et al.* [8]. With this technique, SPP resonance can be achieved at normal or near-normal incidence, permitting

Manuscript received May 03, 2011; accepted June 21, 2011. Date of publication July 14, 2011; date of current version December 07, 2011. This work was supported in part by the DARPA Center for Optofluidic Integration and by SPAWAR Systems Center Pacific. The associate editor coordinating the review of this paper and approving it for publication was Dr. Dwight Woolard.

J. Ptasinski is with the Department of Electrical and Computer Engineering, University of California at San Diego, La Jolla, CA 92093-0407 USA, and also with the SPAWAR Systems Center Pacific, San Diego, CA 92152 USA (e-mail: jptasins@ucsd.edu; Joanna.ptasinski@navy.mil).

L. Pang, P.-C. Sun, B. Slutsky, and Y. Fainman are with the Department of Electrical and Computer Engineering, University of California at San Diego, La Jolla, CA 92093-0407 USA (e-mail: lpang@ece.ucsd.edu; pangchens@yahoo.com; bslutsky@ucsd.edu; fainman@ece.ucsd.edu).

Color versions of one or more of the figures in this paper are available online at http://ieeexplore.ieee.org.

Digital Object Identifier 10.1109/JSEN.2011.2161605

measurement over a large area not limited by the focal depth of the imaging optics.

The rest of this paper first goes through a short review of the theory and concepts associated with plasmonic detection and differential measurement. Fabrication methods used for the nanohole arrays and the fluidic chambers are then discussed in full detail. Finally, our optical setup, the measurement method and the measurement results for our differential detection scheme are presented.

II. Principles

In our plasmonic nanosensor design, the shape of a DTF curve most closely resembles that of a singly peaked normalized Lorentzian function, which can be described by [8]

$$T_L(\lambda) = \frac{1}{1 + \left(\frac{\lambda - \lambda_0}{\frac{1}{2}w}\right)^2} \tag{1}$$

where λ is the wavelength, λ_0 points to the location where the maximum of the DTF occurs, and w is the parameter specifying the Full Width at Half Maximum (FWHM). The centerpoint λ_0 and the FWHM w of each DTF excited through a nanohole array depend on the permittivity of the metal, the refractive index of the dielectric material, the period of the grating array, and the angle of incidence [9].

The width of the surface plasmon resonance (SPR) DTF curve (the FWHM of the Lorentzian) is directly related to the fill factor of the nanohole array, since a large size hole diameter increases surface wave scattering and broadens the resonance linewidth [8]. Our Rigorous Coupled Wave Analysis (RCWA) simulation results for a 1-D gold nanohole array show a 72% decrease in the FWHM of DTF when the gold fill factor is increased from 0.5 Λ to 0.9 Λ. It should be noted that while small diameter holes give rise to a narrow FWHM, they are difficult to fabricate and they also do not allow for much light to pass through the array in the transmission regime ensuing in a lower intensity signal. For our experiment, we chose the gold fill factor to be 60% as a tradeoff between signal transmission and sharpness of the DTF. However, other fill factors can also be used, depending on the desired gain and linear range of the feedback signal and the noise floor of the detection system. For example, an 85% fill yields (according to our RCWA simulations) 2.35 times narrower DTFs in Fig. 1(b) than a 60% fill, and hence 2.35 times steeper differential slope in Fig. 1(c), but it would also reduce transmitted intensity by a factor of 2.5.

As noted, wavelength and angular interrogation methods require multiple measurements of the DTF, which increases measurement time. Our approach involves just two measurements, one for each of the two DTFs T_1, T_2, corresponding to distinct angles of incidence, and the construction of their difference T_1-T_2. Unlike the individual DTFs, the difference signal crosses zero [Fig. 1(c)] and this location of zero crossing depends only on the locations of the DTFs and not on their magnitude and width. The difference signal also has a greater linear range than the individual DTFs. Both these features are advantageous in a measurement system that tracks the zero crossing with a closed-loop controller.

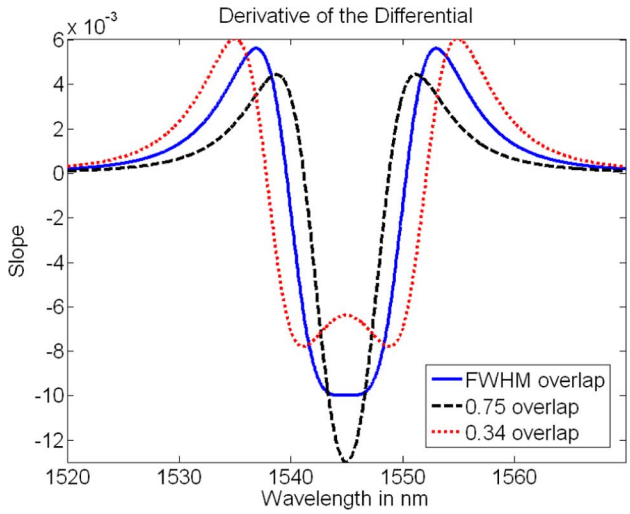

Fig. 2. Derivative of the DTF differential $T_D = T(\lambda_1) - T(\lambda_2)$ when the DTF curves are overlapped at the 0.5 transmittivity value (smooth curve), 0.75 value (dashed line), and the 0.34 point (dotted line).

When the two Lorentzians T_1, T_2 are centered respectively at wavelengths λ_1, λ_2,the slope $\partial(T_1 - T_2)/\partial\lambda$, which is a measure of the linear region of the difference between two DTFs, is expressed as

$$T_D'(\lambda)|_{\lambda_1 - \lambda_2} = \frac{\partial}{\partial\lambda}\left[\left(1 + \left(\frac{\lambda - \lambda_1}{\frac{1}{2}w}\right)^2\right)^{-1} - \left(1 + \left(\frac{\lambda - \lambda_2}{\frac{1}{2}w}\right)^2\right)^{-1}\right]. \tag{2}$$

This slope is plotted in Fig. 2 for various separations between the center of T_1 and T_2. In a closed-loop control system, a steep slope improves measurement sensitivity, while a wider linear region is desirable to make the controller more robust. Fig. 2 illustrates the tradeoff between these two parameters. In the present work, we chose λ_1–$\lambda_2 = \mathrm{FWHM}$ as a reasonable compromise.

Differential detectors have long been utilized in confocal microscopy [10], [11], range finding [12], etc. An advantage of differential measurement is the unique property of self-referencing for optical source fluctuation, since any fluctuation of the intensity will impact the adjacent DTFs equally and thus cancel itself. This concept has been widely adapted by the telecommunication industry, where differential signals are used to carry the bits that eliminate the cause of "ground" noise.

III. Experimental Setup

The samples were fabricated using holographic lithography, where two interfering UV laser beams were incident upon negative MicroChem SU8 photoresist placed on top of a 1.2 mm thick SiO_2 substrate. In order to achieve a hole pattern, each sample was exposed and then rotated 90° for an additional exposure step [13]. Prior to the exposure, the SiO_2 substrate was cleaned in a Pirahna bath (1:1:5 of H_2O:H_2O_2:H_2SO_4) solution for 30 min and the surface was dehydrated by baking on a hot plate at 200 °C for 5 min. A 2 μm layer of SU8-5 was spin deposited at 3000 rpm. The samples were exposed with a Coherent Innova 300 Argon-Ion laser centered at 364 nm with a

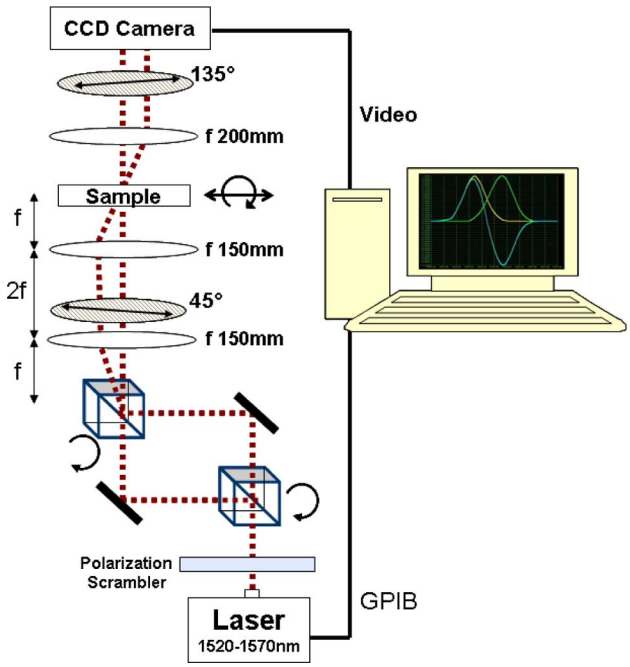

Fig. 3. The differential setup used to measure SPR response to different concentration ethylene glycol solutions.

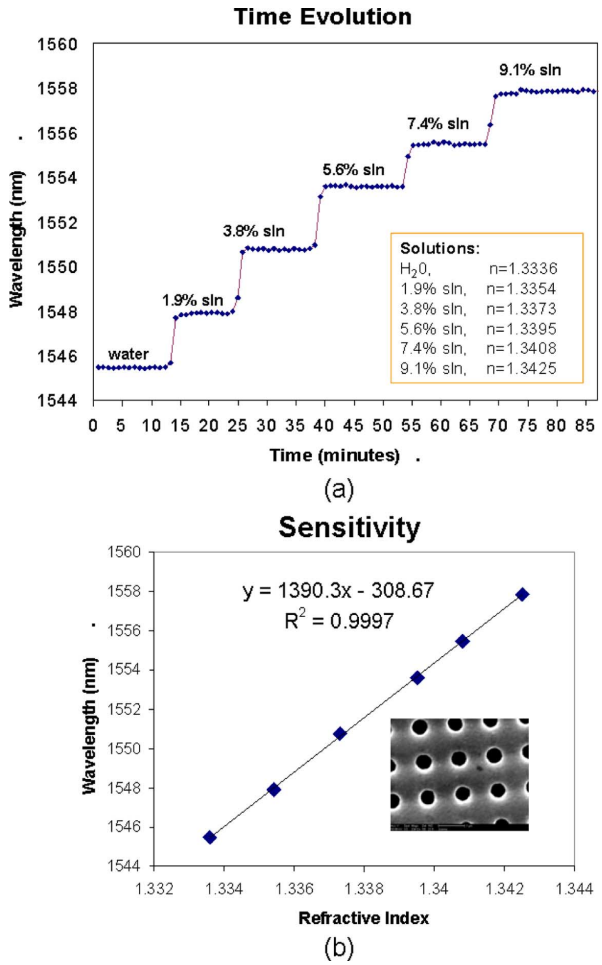

Fig. 4. Evolution of the SPP differential detection spectral response as a function of time. (a) Different concentrations of ethylene glycol are introduced at various time intervals. (b) A linear fit of the time evolution measurement, where the sensitivity is represented by the slope. In this case, the sensitivity is 1390 nm/RIU, and the grating period is 1400 nm.

150 mJ dosage per exposure, and followed by a convection oven soft bake for 1 min. The SU8 development time was 3 min and it was followed by an IPA rinse. A 5 nm thick titanium adhesion layer, followed by a 100 nm gold layer was sputtered onto the samples using the Denton Discovery 18 Sputter System. Fluidic chambers made of Polydimethylsiloxane (PDMS) were affixed on top of each sample's grating array using oxygen plasma [14]. It should be noted that PDMS does not readily bond to Au, hence a region of bare SiO_2 was left on each sample, surrounding the 4 cm^2 gold grating array, in order to facilitate in the PDMS adhesion. The main portion of the fluidic chamber was 13 mm-by-2 mm in size, allowing for both beams to be easily directed onto the grating portion of the sample.

The experimental setup, as shown in Fig. 3, consisted of a tunable New Focus laser in a range of 1520–1570 nm connected to a polarization scrambler in order to randomize the polarization state of input light and to minimize polarization dependent loss associated with the components of the experimental setup. In order to perform the differential measurement, the collimated beams incident at different angles need to meet at the same spot on the sample. This is accomplished by using two polarization independent beam splitters positioned in a Mach–Zehnder configuration, where two beams separated by the first splitter are multiplexed at the same spot onto the second splitter; then both beams from the second splitter are imaged with a 4-F telecentric imaging system on to the sample surface, where the relative angle between the two beams can be fine adjusted by rotation of the second beam splitter. Equivalent beam path lengths ensured spots from the two beams to be equal sized. To further ascertain similar spot sizes, each spot is normalized. Light emerging from the sample is then spatially Fourier transformed by a lens into two parallel beams, where each one is receipted by a photodetector for the differential measurement. In lieu of a pair of detectors, we used an Indigo Merlin CCD camera to record light from the two beams and thus obtain the DTFs corresponding to the two angles of incidence at the sample. The differential signal was then calculated by the computer. A pair of polarizers was placed with one element in front and one element behind the sample, where their polarization state was set to a cross position, to suppress directly transmitted light (nonresonant transmission) and isolate the observation of SPP resonance [8]. The sample along with the microfluidic delivery system was mounted on a rotational stage. Prior to measurement, the laser wavelength was set to 1545 nm and the sample was rotated to obtain equal power in the two detectors. In this way, $\lambda = 1545\,\mathrm{nm}$ was positioned midway between the maxima of the two DTFs at the zero-crossing of the differential signal [Fig. 1(c)]. Detector output was then monitored while fluids of varying refractive indices were introduced into the fluidic channel. Before a measurement was performed, methanol was advanced into the PDMS chamber in order to clean the sample. H_2O was used to flush the methanol and various concentrations of an ethylene glycol solution, ranging from 1.9% to 9.1%, were introduced into the chamber. The measurement process was automated via a Labview program with a GPIB interface to the New Focus tunable laser and video grabbing card to the CCD.

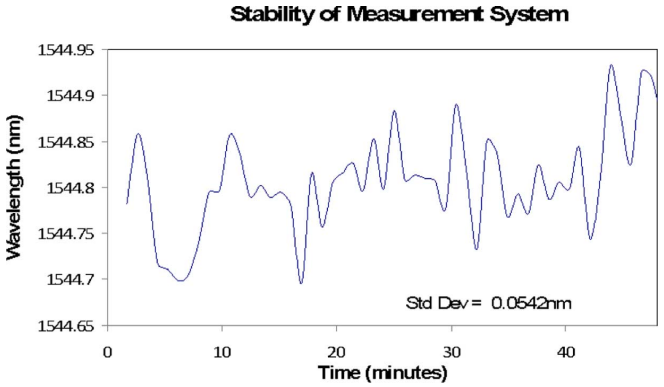

Fig. 5. Stability of the differential measurement system.

IV. Results and Discussion

Fig. 4 reports the results of an experiment in which six different ethylene glycol/water solutions were sequentially introduced into the fluidic chamber. The refractive indices of the solutions, measured separately with a refractometer, are indicated in the inset in Fig. 4(a). Throughout the test, the laser wavelength was continuously adjusted to track the zero-crossing of the differential signal by maintaining equal power in the two detectors. The zero-crossing wavelength is plotted in Fig. 4(a) as a function of time, and in Fig. 4(b) as a function of the refractive index of the fluid. From the linear curve fit in Fig. 4(b), the sensitivity figure $S_\lambda \equiv d\lambda/\mathrm{dn} = 1390\ \mathrm{nm/RIU}$. This is consistent with the analytical expression given by Pang *et al.* [9] for plasmonic mode (1, 0) and grating period close to 1400 nm.

The noise floor and long-term stability of our system is illustrated in Fig. 5, which shows the evolution of the zero-crossing wavelength over 48 min, while maintaining the same material (DI water) in the fluidic chamber. The RMS of fluctuation in Fig. 5 is 0.0542 nm corresponding to a fluctuation in the refractive index of $\Delta n = 4 \times 10^{-5}$ RIU. The noise could be partly due to variation of ambient temperature (the change in the refractive index of water is $\Delta n/\Delta T = 10^{-4}$ RIU/K [15]), and may be reduced by tighter environmental control.

V. Summary

We presented a differential measurement technique for a nanoplasmonic sensor operating in the transmission regime. The differential technique provides an increase in the dynamic range of intensity due to the contribution of the second DTF, it decreases the measurement time due to the tracking of just the zero crossing point, in addition to extending the dynamic range and signal-to-noise ratio. The differential DTF intensity measurement can be amplified by controlling the resonance FWHM, where a narrower FWHM translates into a steeper differential slope. We bypassed the cumbersome Center of Mass (CoM) and only used smoothing for our experiment, where we achieved detection resolution on the order of 10^{-5} RIU. The sensitivity can be improved by increasing the fill factor of the nanohole array at the expense of a reduction in the signal level.

References

[1] C. Lausted, Z. Hu, and L. Hood, "Quantitative serum proteomics from surface plasmon resonance imaging," *Molecular Cellular Proteomics*, pp. 2464–2474, 2008.
[2] C. Shaffer, "Naked proteomics," *Genomics and Proteomics*, vol. 7, pp. G6–G7, 2007.
[3] J. Homola, "Surface plasmon resonance sensors for detection of chemical and biological species," *Chem. Rev.*, vol. 108, pp. 462–493, 2008.
[4] N. Blow, "Proteins and proteomics: Life on the surface,," *Nature Methods*, vol. 6, pp. 389–393, 2009.
[5] R. Slavik and J. Homola, "Ultrahigh resolution long range surface plasmon-based sensor," *Sens. Actuators B*, vol. 123, pp. 10–12, 2007.
[6] X. Y. Yang, D. M. Liu, W. C. Xie, and C. F. Li, "High sensitivity sensor based on surface plasmon resonance enhanced lateral optical beam displacements," *Chin. Phys. Lett.*, vol. 24, pp. 458–461, 2007.
[7] A. Naimushin, S. D. Soelberg, D. U. Bartholomew, J. L. Elkind, and C. E. Furlong, "Portable surface plasmon resonance (SPR) sensor system with temperature stabilization," *Sens. Actuators B: Chem.*, vol. 96, pp. 253–260, 2003.
[8] K. Tetz, L. Pang, and Y. Fainman, "High-resolution surface plasmon resonance sensor based on linewidth-optimized nanohole array transmittance," *Opt. Lett.*, vol. 31, pp. 1528–1530, 2006.
[9] L. Pang, G. Hwang, B. Slutsky, and Y. Fainman, "Spectral sensitivity of two-dimensional nanohole array surface plasmon polariton resonance sensor," *Appl. Phys. Lett.*, vol. 91, pp. 123112–123112, 2007.
[10] Y. Fainman, E. Lenz, and J. Shamir, "Optical profilometer: A new method for high sensitivity and wide dynamic range," *Appl. Opt.*, vol. 21, pp. 3200–3208, 1982.
[11] W. Zhao, R. Sun, L. Qiu, and D. Sha, "Laser differential confocal ultra-long focal length measurement," *Opt. Exp.*, vol. 17, pp. 20051–20062, 2009.
[12] T. R. Corle, J. T. Fanton, and G. S. Kino, "Distance measurements by differential confocal optical ranging," *Appl. Opt.*, vol. 26, pp. 2416–2420, 1987.
[13] L. Pang, W. Nakagawa, and Y. Fainman, "Fabrication of 2-D photonic crystals with controlled defects by use of multiple exposures and direct-write," *Appl. Opt.*, vol. 42, pp. 5450–5456, 2003.
[14] A. Groisman, S. Zamek, K. Campbell, L. Pang, U. Levy, and Y. Fainman, "Optofluidic 1×4 switch," *Opt. Exp.*, vol. 16, pp. 13499–13508, 2008.
[15] I. Thormählen, J. Straub, and U. Grigull, "Refractive index of water and its dependence on wavelength, temperature, and density," *J. Phys. Chem. Ref. Data*, vol. 14, pp. 933–945, 1985.

Joanna Ptasinski received the M.Sc. degree in electrical engineering from San Diego State University, San Diefo, CA, in 2006, where she investigated two-dimensional photonic crystal waveguides and the guiding mechanism associated with the structures. Currently, she is working towards the Ph.D. degree in photonics at the University of California San Diego, La Jolla, where she is a recipient of the DoD SMART Scholarship.

Since 2002, she has worked at SPAWAR Systems Center Pacific (SSC-Pac). She also holds 11 patents stemming from her research at SSC-Pac.

Lin Pang received the Ph.D. degree in optical recording material and microfabrication from Sichuan University, Sichuan, China, in 1998.

He was a Research Fellow at Tsinghua University, China, between 1999 and 2000, where he developed an inorganic-organic recording material. Since 2001, he has been with the Ultrafast and Nanoscale Optics Group, University of California at San Diego, La Jolla. As a Research Scientist, his current interests include hybrid holographic lithography, micro, nanofabrication, nanofluidics, and biosensors based on surface plasmon resonance at nanoresonators.

Pang-Chen Sun received the M.Sc. degree in electrical engineering and the Ph.D. degree in mechanical engineering from University of Michigan, Ann Arbor.

After graduation, he continued his research work in optical information procession and communication at the University of California, San Diego (UCSD). He has authored and coauthored more than 50 journal published research papers and also holds six patents. He has also worked in the optical/photonic industry to develop various communication and sensing products. He is currently working as a member of the Senior Technical Staff at the UCSD Calit2 Center.

Boris Slutsky received the Ph.D. degree from the University of California, San Diego (UCSD), in 1998.

He has held senior engineering positions at several private companies and the position of Ames Associate at NASA Ames Research Center, Moffett Field, CA. He returned to UCSD in 2006 as a Principal Development Engineer at the California Institute for Telecommunications and Information Technologies.

Yeshaiahu Fainman received the M.Sc. and Ph.D. degrees from Technion - Israel Institute of Technology, Haifa, Israel, in 1979 and 1983, respectively.

He is a Cymer Professor of Advanced Optical Technologies in Electrical and Computer Engineering at the University of California, San Diego (UCSD). Since 1990, he has been directing research of the Ultrafast and Nanoscale Optics Group at UCSD and helped to make pioneering contributions to utilizing near-field optical phenomena in inhomogeneous and meta-materials, nanophotonics and plasmonics, nonlinear optics of femtosecond pulses, and nonconventional imaging. His research applications target information technologies and biomedical sensing. He has past experience in leading large-scale multidisciplinary projects. For example, in the early 1990s, he was a Director of a project on "Photonic Imaging Networks," supported by Focused Research Initiative program of BMDO, led as a Director one of the DARPA OptoCenters (Optofluidics), DARPA's Si Phaser and NACHOs programs, and he is currently a Deputy Director of NSF's Engineering Research Center -CIAN. He contributed over 200 manuscripts in peer review journals and over 350 conference presentations and conference proceedings. His current research interests are in near-field optical science and technology compatible with CMOS manufacturing. Specific research projects include: (i) design, fabrication and experimental validation of nanoscale resonant optical structures and devices exploiting both dielectric and metalo-dielectric nanostructures; (ii) nanoscale lasers and evanescent field imaging and sensing; (iii) plasmonic nanostructures for electromagnetic field localization beyond diffraction limit, enabling biomedical sensing and imaging on the nanoscale in all three spatial dimensions; (iv) optofluidics technology integrating microfluidics with micro and nanoscale optics for sensing and monitoring; (v) optical signal and information processing using femtosecond laser pulses; (vi) quantum cryptography, communication, and quantum information processing; and (vi) multidimensional quantitative imaging in near and far fields.

Prof. Fainman is a Fellow of the Optical Society of America, Fellow of the Institute of Electrical and Electronics Engineers, and Fellow of the Society of Photo-Optical Instrumentation Engineers. He is a recipient of the Miriam and Aharon Gutvirt Prize, Technion, Haifa, Israel (1982), the Lady Davis Fellowship (2006), and Brown Award (2006).